Bio-Design and Manufacturing (2018) 1:45–61
https://doi.org/10.1007/s42242-018-0006-1

REVIEW

# 3D bioprinting for cell culture and tissue fabrication

Honglei Jian[1] · Meiyue Wang[1] · Shengtao Wang[1] · Anhe Wang[1] · Shuo Bai[1]

Received: 9 January 2018 / Accepted: 27 January 2018 / Published online: 26 February 2018


**Abstract**
Three-dimensional (3D) bioprinting is a computer-assisted technology which precisely controls spatial position of biomaterials, growth factors and living cells, offering unprecedented possibility to bridge the gap between structurally mimic tissue constructs and functional tissues or organoids. We briefly focus on diverse bioinks used in the recent progresses of biofabrication and 3D bioprinting of various tissue architectures including blood vessel, bone, cartilage, skin, heart, liver and nerve systems. This paper provides readers a guideline with the conjunction between bioinks and the targeted tissue or organ types in structuration and final functionalization of these tissue analogues. The challenges and perspectives in 3D bioprinting field are also illustrated.

**Keywords** 3D bioprinting · Bioink · Cell culture · Tissue fabrication · Organoid

## Introduction

Three-dimensional (3D) bioprinting, a computer-assisted technology, is able to precisely control spatial position of biomaterials, growth factors and living cells with an ultimate goal of creating functional tissues and organs [1,2]. 3D bioprinting is becoming more and more popular in tissue fabrication because of its capacity of using customized structures and autologous cells to directly produce complex and biomimetic tissue architectures [3,4]. During printing process, the biomaterials made for living cells that behave much like a liquid allowing to "print" into a desired shape, are called bioinks. 3D bioprinting technology offers unprecedented possibility to bridge the gap between structurally mimic tissue constructs and functional tissues or organoids [5–7].

According to the employed printing mechanisms, the bioprinting techniques for tissue fabrication are classified into three main types: extrusion-, droplet- and laser- based bioprinting process [8]. In general, extrusion-based bioprinting, perhaps the most widespread method for fabrication, depends on mechanical-, pneumatic- or solenoid-driven micro-extrusion to create continuous strands of bioink [9]. In droplet-based bioprinting, various kinds of energy sources covering thermal, piezoelectric, electrostatic, hydrodynamic, acoustic and microvalve are employed to generate droplets of bioink [10]. In the case of laser-based bioprinting, laser energy is utilized for high-precision deposition of bioinks [11]. These bioprinting processes have their respective printing features and requirements of suitable inks [12], which are summarized in Table 1.

With regard to the fabrication of a desired tissue or organoid, the consideration about the suitable bioink features is far beyond the choice of a suitable bioprinting process. When a biomaterial is printed onto the substrate (i.e., the receiving surface), it needs to undergo a fast phase transition to preserve the shape and resolution, and thereafter maintain cell viability and proliferation during post-printing incubation [13], which is one of the most important features distinguishing injectable and printable hydrogel material [14,15]. The structural and functional diversity of tissue fabrication leads to a wide development of bioink. The major bioink material used in tissue biofabrication and 3D bioprinting is hydrogel matrix and usually nature-derived. It is because of that high-water content of hydrogel, up to 1000 times of their original weight in aqueous media [16], enables well penetration of oxygen, nutrients, growth factors and other water-soluble components, thereby making them very suitable for tissue or organoid fabrication [17].

Honglei Jian and Meiyue Wang have contributed equally to this work.

✉ Shuo Bai
baishuo@ipe.ac.cn

[1] State Key Laboratory of Biochemical Engineering, Institute of Process Engineering, Chinese Academy of Sciences, Beijing 100190, China

**Table 1** Types and features of bioprinting techniques [8,12]

| Types of bioprinting | Extrusion-based | Droplet-based | Laser-based |
|---|---|---|---|
| Requirements of bioink | Viscosity $< 6 \times 10^7$ mPa s, shear thinning, thixotropic behavior, low surface tension and adhesion, rapid gelation, shape retention | Viscosity $< 15$ mPa s, rheopectic behavior, nonfibrous nature, medium surface tension, rapid gelation | Viscosity $< 300$ mPa s, viscoelasticity, intermediate adhesion, low surface tension, absorption of laser kinetic energy, rapid gelation |
| Requirements of substrate | Wettability, high surface roughness | Wettability, high surface roughness, induces viscous forces | Wettability, high surface roughness, induces viscous forces |
| Printing speed | Slow | Medium | Fast |
| Cell density | High, spheroids | $< 10^6$ cells/mL | $< 10^8$ cells/mL |
| Post-printing cell viability | $\sim 80\%$ | $> 85\%$ | 95% |
| Cost | Medium | Low | High |

Recent advances in bioink materials for constructing 3D cell environments have greatly promoted the development of tissue engineering. The printability of the biomaterials heavily relies on their inherent mechanical properties such as rheological properties [18–20], bioactive moieties [21,22] and degradation behavior. For instance, the rheological properties of a bioink have a direct influence on printability, compatibility, shear stress yielded by cell encapsulation, as well as structural integrity and resolution of 3D printed construct [23]. The gelation process of a bioink matrix has a crucial role in both the resolution and cell viability [24]. Furthermore, the mechanical properties and degradation behavior not only affect cell growth, proliferation and differentiation, but also long-term biocompatibility in the fabricated tissues [25–28].

Although 3D bioprinting has made some attractive progress in tissue fabrication, this technique has not yet been used to make a lab-to-clinic translation. This paper reviews the recent progresses in 3D bioprinting from the perspective of tissue and organoid biofabrication. When planning for bioprinting, one should first consider the microenvironment characteristics and cell types of the targeted tissue or organ, and thereafter choose suitable bioink materials and a rational printing strategy. Therefore, we briefly focus on the diverse bioinks used for biofabrication of tissues and organoid including blood vessel, bone, cartilage, skin, heart, liver and nerve. The paper provides readers a guideline with the conjunction between bioinks and the targeted tissue or organ types in structuration and final functionalization of these tissue analogues. The challenges and perspectives in 3D bioprinting field are also illustrated.

## Bioprinting of blood vessel

The vascular networks exist in almost all organs of the human body, playing crucial roles in nutrient transport and waste removal. Blood vessels mainly consist of endothelial cells (ECs), smooth muscle cells (SMCs) and fibroblasts. In artificial organs, vasculature formation has always been an impenetrable barrier in tissue engineering [29]. There are several difficulties in the complication of artificial vessels, such as scaled-up vessels [30]. The dimension of synthetic organs is around hundreds of millimeters which is the maximum distance the substances could reach and hence they need vasculature to transfer nutrients, oxygen and wastes [31]. Imperfect vascularization could lead to necrosis and high morbidity of the developed organoids [32]. Therefore, building a mature and perfect vascular network, especially in the field of the functional organoid fabrication, is an urgent and desired target.

When planning to fabricate a vessel-like construct, a fully understanding and mimicking of the environment and component of the native blood vessels is of importance. As summarized in Table 2, the vascularization strategies by bioprinting technique have been widely studied. Researchers utilized biocompatible and biodegradable materials to print vascular-like structures with micron-sized diameters for cell adhesion, proliferation, differentiation and migration [33,34]. Xu et al. employed a platform-assisted 3D inkjet bioprinting system to fabricate zigzag tube structure, in which fibroblast retained cell viability of above 80% in 3 days of culture. The results illustrated that vessel-like construct with complex geometry could be successfully fabricated by 3D bioprinting technique [35]. Miller et al. [36] constructed a rigid filament network using endothelial cells encapsulated within carbohydrate glass (Fig. 1a). In the circumstance, the bioprinted scaffold was perfused with blood under high-pressure pulsating flow, and the cells retained a high vitality in the vessel-like architecture [36].

In a study by Bertassoni et al. 3D microchannel networks were developed containing mouse calvarial pre-osteoblasts cells (MC3T3) and human umbilical vein endothelial cells (HUVECs). In particular, the functions of the gelatin methacrylate (GelMA) scaffold in mass transport, cell via-

**Table 2** Bioinks for bioprinted blood vessels

| Bioink materials | Cell sources | Printing types | Culture time | Outcomes |
|---|---|---|---|---|
| Alginate | Murine fibroblasts (NIH 3T3) | Droplet-based | 3 days | Constructing a tubular overhang structure with the cell viability of 80% [35] |
| Carbohydrate glass, poly (ethylene glycol), fibrin, Matrigel, alginate, agarose | HUVECs | Extrusion-based | 9 days | Fabricating a vessel-like architecture perfusable with blood under high-pressure pulsatile flow [36] |
| GelMA, agarose | MC3T3, HUVECs | Extrusion-based | 14 days | Formation of endothelial monolayers within the fabricated vascular networks [37] |
| Matrigel, agarose | ECs | Laser-based | 11 days | Creation of a tubular structure with a diameter of 17 mm and a wall thickness of 2 mm [38] |
| GelMA | NIH 3T3 | Extrusion-based | 8 days | Fabricating a 5-layers structure and the spheroid size was up to 750 mm [39] |
| Gelatin, hyaluronic acid | NIH 3T3 | Extrusion-based | 3 weeks | Constructing a cellularized tubular structure for cell attachment and proliferation [40] |

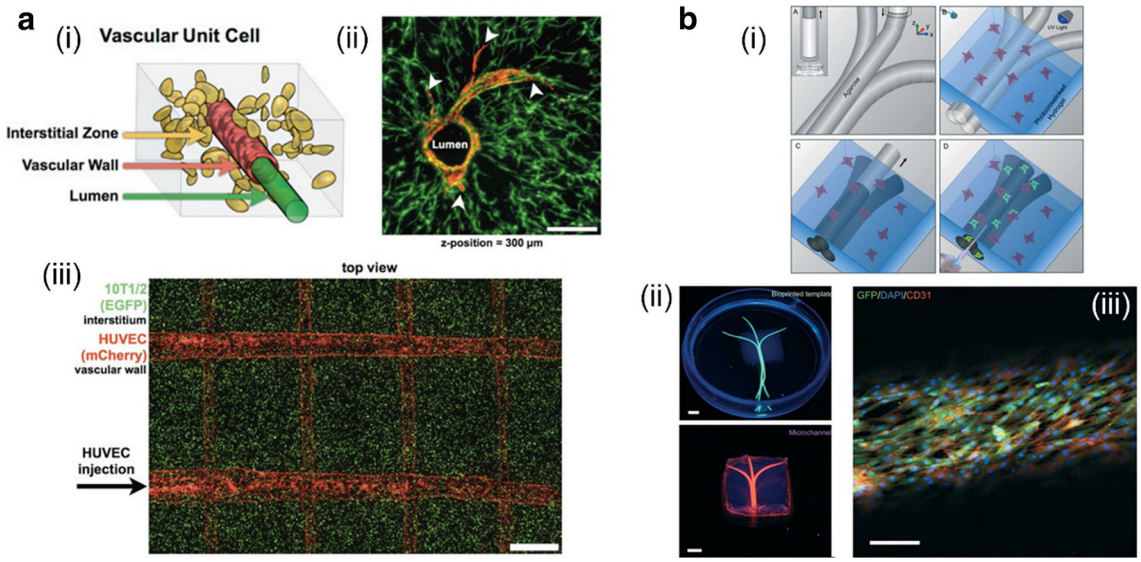


**Fig. 1** 3D bioprinting of blood vessels. **a** The three key elements of vascularized tissues: (i) The structure of vascular unit cell, (ii) Sprouts (arrowheads) were formed by endothelial cells; the optical thickness of the vascular-like structure was 200 μm, (iii) The bioprinted vascular was formed by 10T1/2 cells and HUVECs; 10T1/2 cells encapsulated in fibrin formed interstitium and HUVECs was injected into the lumen. Scale bars, 1 mm. Reproduced with permission [36]. Copyright 2012 Springer Nature. **b** The structure of bioprinted hydrogels and vascular-like tissue: (i) Schematic demonstration of the microchannels fabricated by template micromolding, (ii) Two-dimensional ramose microchannels encapsulated in GelMA hydrogels were formed by fluorescent microbead. Microchannels diameter, 500 μm; Scale bars, 3 mm, (iii) Confocal image of monolayer channel formed by HUVECs with GFP/DAPI/CD31 markers. Scale bar, 250 μm. Reproduced with permission [37]. Copyright 2014 Royal Society of Chemistry

bility and differentiation were evaluated (Fig. 1b) [37]. In another work, Fan et al. designed a Matrigel and agarose hybrid hydrogel system, where the former was used as microenvironment for cell growth, and the latter undertook the duty for maintaining the 3D printed tubular structure. It was demonstrated that human epithelial cells encapsulated within the constructs showed high cell viability and favorable cell spreading morphology [38]. Bertassoni et al. fabricated a 5-layers structure based on GelMA laden with NIH 3T3, and in this system the spheroid size was up to 750 mm after 8 days of culture [39]. Skardal et al. [40] utilized photo-crosslinkable hyaluronan-gelatin hydrogels for two-step bioprinting of a cellularized tubular structure, in which cell attachment and proliferation of NIH 3T3 were studied.

## Bioprinting of bone

The skeleton system provides structural support and functional maintenance for the whole body. The bone tissue is mainly composed of inorganic mineral hydroxyapatite (accounting for 70% of bones), water and collagen. As a mineral reservoir, bone can maintain dynamic homeostasis in the bone marrow, support muscular contraction and reduce damage from outer surroundings [41]. Notably, collagen and mineral play critical roles in tenacity and stiffness of bone, respectively.

The mature bone mainly consists of three types of cells: osteocytes, osteoclasts and osteoblasts. Osteocytes, the most abundant cells in bone tissue, maintain the morphology of bone by forming a 3D network, which can make them act as mechanical sensor [42]. Osteoclasts are responsible for bone resorption. In addition, osteoblasts as secretory cells can form osteoid with abundant collagen [43]. In terms of bone regeneration, considerable energy has been spent on regenerative medicine and surgery, but there are still plenty of limitations. In recent years, 3D printing therapy methods give hopes to the patients suffering bone injury [44,45]. It can recruit patient-specific cells with the biocompatible and biodegradable material to the defect sites. On the other hand, stem cells are widely used in bone engineering due to their capability of self-renewal and differentiation.

As illustrated in Table 3, numerous strategies have been developed for bioprinting of bone-like tissue. Fedorovich et al. utilized alginate hydrogel laden with endothelial progenitors and bone marrow stromal cells to print a vascularized bone graft in which the cells could retain viability and differentiate toward lineage [46]. Gruene et al. [47] employed a computer-aided laser printing technology to create a grid pattern with mesenchymal stem cells (MSCs) encapsulated within alginate. The results provided the foundation of a 3D stem cell-laden hydrogel structure with variable differentiation levels [47]. Byambaa et al. fabricated a bone-like architecture where hMSCs, HUVECs and vascular endothelial growth factor (VEGF) were embedded within GelMA. It is illustrated in Fig. 2a that hMSCs differentiated into perivascular cells in co-culture with HUVECs at day 7, forming a stabilized vasculature in the bone-like construct [48]. Based on the in vitro researches of 3D bioprinting for tissue engineering, Keriquel et al. in situ printed MSCs-laden nano-hydroxyapatite and collagen bioinks in calvaria defec-

**Table 3** Bioinks for bioprinted bones

| Bioink materials | Cell sources | Printing types | Culture time | Outcomes |
|---|---|---|---|---|
| Alginate | MSCs | Extrusion-based | 2 weeks | Printing a vascularized bone graft with the cell viability of 86% [46] |
| Alginate | MSCs | Laser-based | 25 days | Constructing a grid pattern and the size of spheroid could arrived in 1mm [47] |
| GelMA | hMSCs, HUVECs | Extrusion-based | 21 days | Fabricating microstructured bone-like tissue containing a perfusable vascular lumen [48] |
| Collagen, nano-hydroxyapatite | MSCs | Laser-based | 11 days | Cellular arrangements had obvious impacts on bone tissue regeneration [49] |
| Matrigel, alginate | Endothelial progenitors, multipotent stromal cells | Extrusion-based | 2 weeks | Cell differentiation in the printed porous structures led to expected bone tissue formation [50] |
| Agarose | NIH 3T3 | Extrusion-based | 3 days | Successfully bioprinting of a cell-gradient pattern [51] |
| Decellularized bone matrix, PCL | hASCs | Extrusion-based | 3 weeks | The scaffolds were implanted into murine calvarial defects and yielded bone regeneration [52] |

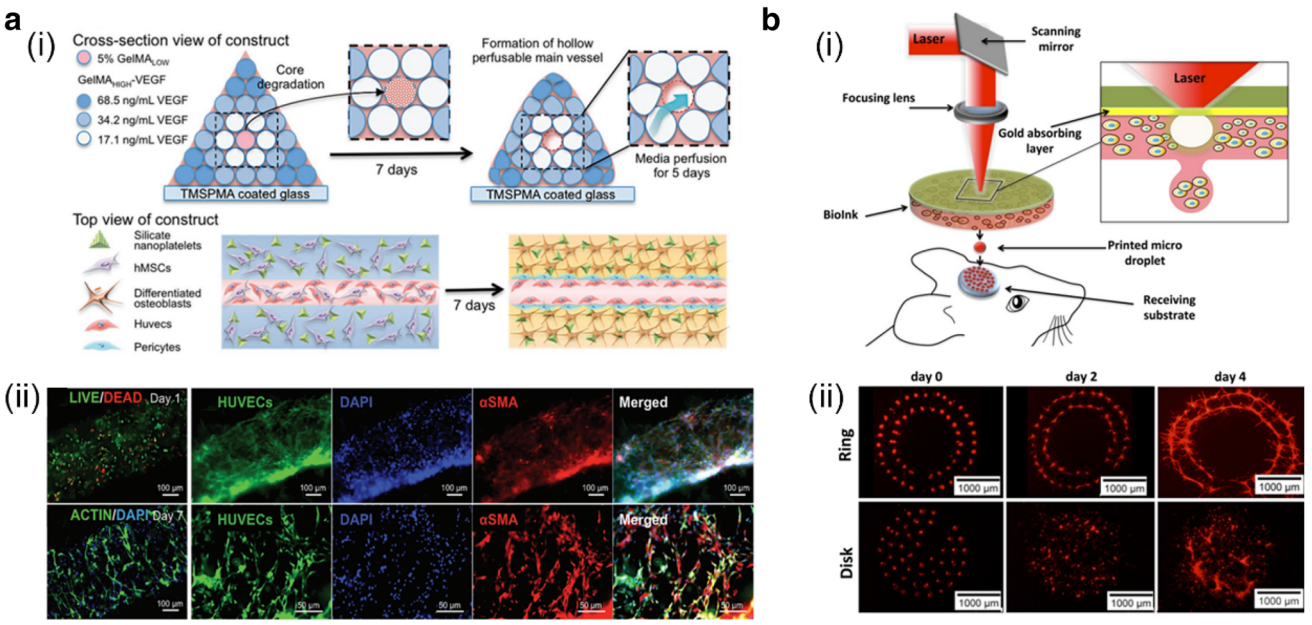


**Fig. 2** 3D bioprinting of bones. **a** Bone tissue bioprinting strategy and fluorescence image of the bioprinted vascular network in a single GelMA fiber: (i) Bone-like tissue architecture containing GelMA, hMSCs, HUVECs and VEGF was accomplished by complex procedures, (ii) Formation of a stabilized vasculature in a 3D bioprinted construct by hMSCs differentiation into perivascular cells in co-culture with HUVECs at day 1 and day 7. Reproduced with permission [48]. Copyright 2017 John Wiley and Sons. **b** Schematic representation of the laser assisted bioprinting and the fluorescence images of ring and disk patterns: (i) Mice with defect calvaria experienced in situ treatment which was accomplished by laser assisted bioprinting, (ii) The influence of different printing patterns on cells performance was shown in the fluorescence images at days 0, 2 and 4. Scale bars, 1000 μm. Reproduced with permission [49]. Open Access

tive mice. Different geometries were printed on the defect of mouse. The results showed that cellular arrangements had obvious impacts on bone tissue regeneration (Fig. 2b) [49].

Fedorovich et al. printed intricate porous constructs containing endothelial progenitors and multipotent stromal cells embedded within Matrigel and alginate [50]. It was found that bone-like tissue was formed in the multipotent stromal cell-laden part of the printed grafts after subcutaneous implantation in mice [50]. Carlier et al. successfully bioprinted bone constructs with cell-gradient patterns. NIH 3T3 cells were encapsulated in agarose with varying cell densities and retained a high cell viability for 3 days post-fabrication [51]. Hung et al. used decellularized bone matrix and polycaprolactone (PCL) laden with human adipose-derived stem cells (hASCs) as bioinks for craniofacial regeneration. When the hybrid scaffold implanted into critical-sized murine calvarial defects, the enhanced bone regeneration was observed [52].

## Bioprinting of cartilage

The cartilage is extensively found in joints of bone, nose and ear acting as a semi-rigid connective tissue. According to the different contents of collagen and proteoglycan which are the main components of the extracellular matrix (ECM), cartilage can be divided into three types: hyaline cartilage, elastic cartilage and fibrous cartilage [53]. Among those, hyaline cartilage is closely related to the skeletal system [54]. The self-repairing capacity of cartilage is very limited, because of the absence of vascular, neural or lymphatic structures [55]. Therefore, cartilage damage is very difficult to heal. Osteoarthritis is a common chronic musculoskeletal disease caused by degradation of articular cartilage. As a chronic and refractory disease, it brings the patients unbearable pain and reduced life quality.

In the past few years, researchers adopted joint replacement surgery to treat arthritis, but the difficulties and costs of this method were too high [56]. Nowadays, although tissue engineering emerges and aims at cartilage regeneration by fabricating cell-laden structures [57], it cannot fabricate a cartilage tissue as the same as the native one due to its complicated structures and specific characters. In order to overcome these limitations, 3D bioprinting system was developed to mimic the natural microenvironment of tissue and successfully used in reconstruction of cartilage tissues. As shown in Table 4, chondrocytes are the optimal cell type for cartilage fabrication, since they are main cells in a special microenvironment assembled by structural and functional proteins in cartilage tissue [58]. Additionally, stem cell is an alternative cell source for cartilage biofabrication attributing to its differentiation ability.

**Table 4** Bioinks for bioprinted cartilages

| Bioink materials | Cell sources | Printing types | Culture time | Outcomes |
|---|---|---|---|---|
| GelMA | Chondrocytes | Extrusion-based | 4 weeks | Fabricating a grid-like structure with the cell viability of 82% in 3 days of culture [59] |
| Hyaluronic acid | Chondrocytes, osteoblasts | Extrusion-based | 2 weeks | Cell viability of 90%, demonstrating hydrogel-directed cell migration [60] |
| GelMA | BMSCs | Extrusion-based | 28 days | Fabricating a fibrocartilage-like tissue [61] |
| Silk fibroin, gelatin | BMSCs | N/a | 21 days | The printed scaffold showed excellent performance for cartilage repair in a knee joint [62] |
| PCL, alginate | Chondrocytes | Extrusion-based | 4 weeks, | The printed scaffolds showed enhanced cartilage tissue and type II collagen fibril formation in vivo [63] |
| Hyaluronic acid, dextran | Chondrocytes | Extrusion-based | 3 weeks | Forming a semi-interpenetrating network and the cell viability was 86% [64] |
| Cellulose, alginate | Chondrocytes, MSCs | Extrusion-based | N/a | The printed scaffold was transplanted to nude mice and cells in it showed good proliferation [65] |
| Hyaluronic acid | MSCs | Extrusion-based | 21 days | MSCs in the hydrogel showed promising chondrogenic differentiation and viability [66] |
| Collagen | Fibrochondrocytes | Extrusion-based | 10 days | The constructs were mechanically stable and able to support and maintain cell growth [67] |

Schuurman et al. fabricated a grid-like structure, where chondrocytes embedded in GelMA showed the viability of 82% in 3 days of culture [59]. With regard to 3D bioprinting of cartilage tissue, suitable bioinks with high biocompatibility appeared to be particularly important. In view of this, Park et al. utilized hyaluronic acid and type I collagen hydrogels to mimic ECMs of chondrocytes and osteoblasts [60]. It was demonstrated that the hydrogels could direct cell migration, chondrocytes moving to hyaluronic acid, while osteoblasts migrating to type I collagen [60]. Daly et al. [61] aimed to screen out proper hydrogels to induce bone marrow stem cells (BMSCs) to differentiate toward cartilage. The commonly used hydrogels including agarose, alginate, GelMA and BioINK$^{TM}$ were employed to construct cartilage structures. It was found that alginate and agarose were suitable for hyaline-like cartilage fabrication, while GelMA and BioINK$^{TM}$ for the formation of fibrocartilage-like tissue. Moreover, MSCs encapsulated in all the constructs showed the viability of above 80% [61]. As shown in Fig. 3a, in the study by Shi et al. the 3D bioprinted scaffold composed of silk fibroin and gelatin has been successfully in vitro cultured and in vivo applied for cartilage injury repair [62]. In another study displayed in Fig. 3b, the porous 3D scaffold was bioprinted using PCL and alginate laden with chondrocytes [63]. The results indicated the formation of type II collagen and cartilaginous tissue in the printed scaffold.

Pescosolido et al. developed a semi-interpenetrating network based on hyaluronic acid and dextran [64]. Apelgren et al. created a scaffold composed of chondrocytes and MSCs-laden cellulose and alginate hydrogels. The scaffold was then transplanted to nude mice and cells in it showed good proliferation [65]. In another work by Stichler et al. MSCs showed promising chondrogenic differentiation in the hybrid Hydrogels [66]. Furthermore, Rhee et al. [67] developed soft cartilage tissue implants with collagen seeded with primary meniscal fibrochondrocytes, which were able to support and maintain cell growth.

## Bioprinting of skin

The skin is deemed as the largest organ in the human body, which can reach up to a coverage area of 1.5–2 $m^2$ and a weight of 3–10 kg, approximately 15% of an adult's weight [68]. Skin plays a major role in protecting body from external injury, including physical, chemical and UV radiation as well as viral and bacterial infection. Furthermore, skin can regulate the body temperature and water metabolism for homeostasis [69]. The layer-by-layer structure of skin consists of epidermis, basement membrane, dermis and hypodermis from outside to inside. Epidermis is about 0.05 mm thick except the skin of palms and soles of feet, of which the main cell type (approximately 95%) is keratinocytes. Basement membrane connecting epidermis with dermis provides a vital structure for mechanical strength of skin. There are several special components of ECM present in this skin layer, such as collagen, glycoproteins and integrins [70]. Dermis is characterized by abundant blood vessels and ECM secreted by fibroblast, which has ability to percept pain, touch and temperature due to the encapsulated nerve

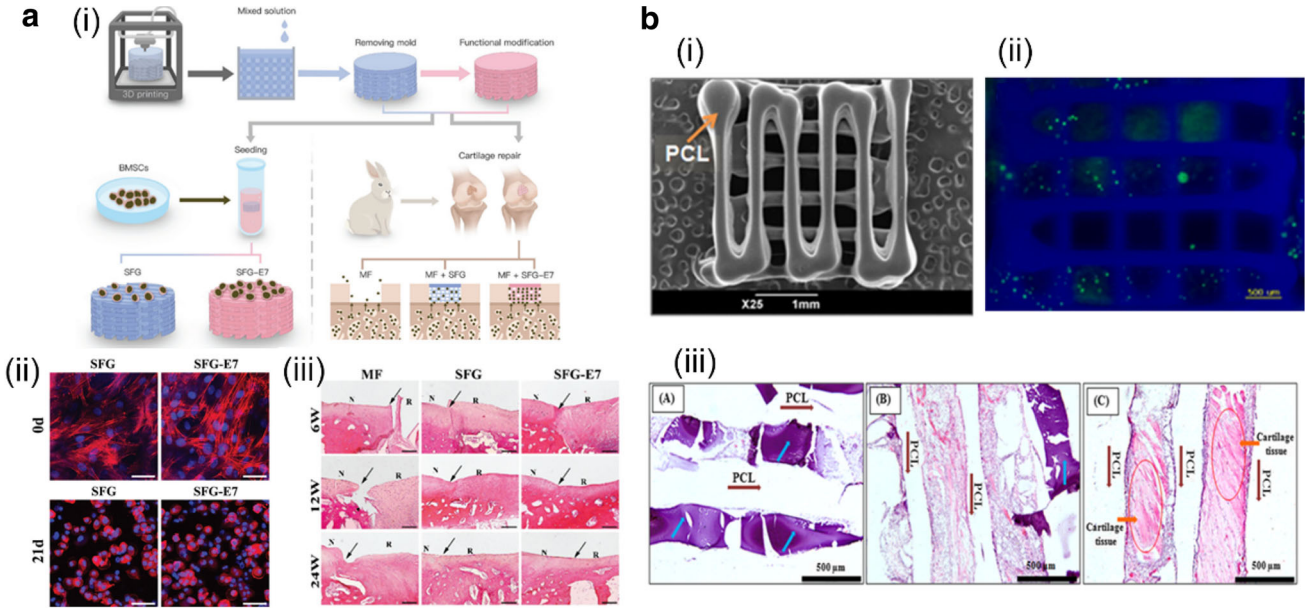


**Fig. 3** 3D bioprinting of cartilage. **a** The culture of 3D bioprinted cartilage tissue in vitro and in vivo: (i) Schematic illustration of 3D printing process, (ii) The morphology of MSCs encapsulated in different hydrogels was observed by Phalloidin/Hoechst staining at day 0 and day 21. Scale bars, 50 μm, (iii) H&E staining of repaired cartilage at 6, 12, and 24 weeks (*N* normal cartilage; *R* repair cartilage; the arrows indicate the margins of the normal cartilage and repaired cartilage). Reproduced with permission [62]. Copyright 2017 John Wiley and Sons. **b** The schematic of the bioprinted scaffold and cartilage-like tissue: (i) SEM images of bioprinted porous 3D PCL scaffold, (ii) Fluorescence microscopy image of the chondrocytes-laden alginate construct; the chondrocytes were marked by live/dead staining. Scale bar, 500 μm, (iii) Histochemical staining for cartilaginous tissue formation; thin microsections of bioprinted implants retrieved from nude mice after 4 weeks were treated by H&E staining. Scale bars, 500 μm. Reproduced with permission [63]. Copyright 2013 John Wiley and Sons

in it. Hypodermis, mainly made of adipocytes and multipotent stem cells, provides various functions of heat insulation, energy storage and resistance of external mechanical forces [71].

However, skin is unable to heal under the situation of serious physical trauma, chemical trauma or genetic defect. The standard treatment for skin injury is based on autologous split-thickness skin grafts, which is not suitable for a large area of injury yet [72]. Although various kinds of skin substitutes are widely developed, there still exist many limitations, such as the cost, functions and biodegradation performance. Recently, reconstruction of skin is achieved by 3D bioprinting technique, as illustrated in Table 5.

In a study by Lee et al. [73], a multi-layered skin tissue was fabricated using collagen laden with human skin fibroblasts and keratinocytes. A poly(dimethylsiloxane) (PDMS) mold was made to simulate the skin wound. High vitality of each cell layer in the PDMS mold indicated that organotypic skin tissue can be fabricated by 3D bioprinting system (Fig. 4a) [73]. Likewise, Vivian Lee et al. constructed a skin-like tissue in which collagen was applied as ECM-mimicking material, keratinocytes and fibroblasts mimicking the epidermis and dermis, respectively. It was demonstrated that cell viability in the skin-like construct was above 90% in 1 week [74]. Moreover, Cubo et al. created a human plasma-based bilayer skin-like tissue containing plasma-derived fibrin, fibroblasts and keratinocytes, which had successfully used for the treatment of burnt, traumatic and surgical wounds in many patients [75]. The results revealed that the printed skin-like tissue, both in vitro culture and in transplantation to immune-deficient mice, showed similar characteristics with human skin [75]. In another study by Pourchet and co-workers in Fig. 4b, the skin tissue was 3D bioprinted and further underwent consolidation and maturation, in which NIH 3T3 was embedded within gelatin, alginate and fibrinogen hydrogels [76]. It was found that the bioprinted skin and normal human skin showed similar optical microscopy images after 26 days of culture.

## Bioprinting of heart

The heart is a muscular organ which pumps blood through the body. The metabolism of the body including oxygen supply, nutrients transport and metabolic waste excretion largely depends on blood flow, which is realized by systole and diastole [77]. Cardiovascular system is an airtight system composed of heart and blood vessel, in which heart offers energy for blood flow and synchronously vessels transfer blood to accomplish the circulation of blood. The heart con-

**Table 5** Bioinks for bioprinted skin

| Bioink materials | Cell sources | Printing types | Culture time | Outcomes |
|---|---|---|---|---|
| Collagen | Fibroblasts, keratinocytes | Droplet-based | 4 days | Creating a multi-layer skin-like tissue [73] |
| Collagen | Fibroblasts, keratinocytes | Droplet-based | 1 week | Keratinocytes were cultured at the air-liquid boundary, which promoted their terminal differentiating into corneocytes [74] |
| Fibrin | Fibroblasts, keratinocytes | Extrusion-based | 17 days | The bioprinted skin implanted in the immunodeficient mice was similar to the native skin after 4-6 weeks [75] |
| Gelatin, alginate, fibrinogen | NIH 3T3 | Extrusion-based | 26 days | Bioprinted skin showed similar structure with normal human skin after 26 days of culture [76] |

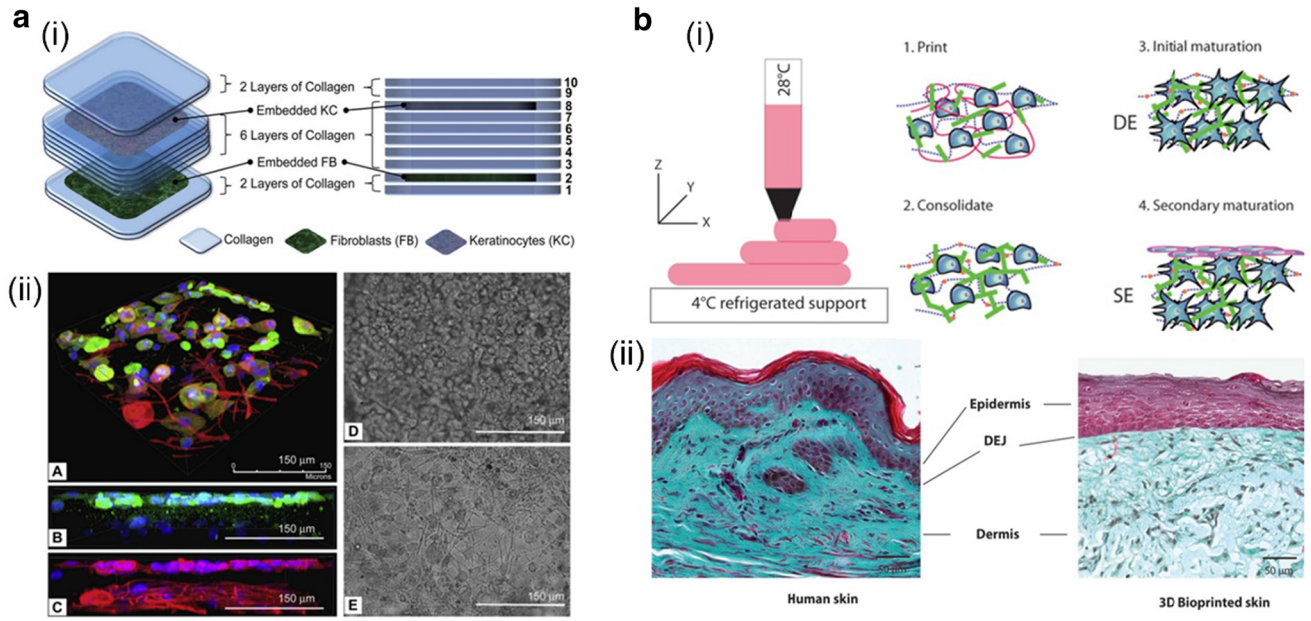


**Fig. 4** 3D bioprinting of skin. **a** Images of schematic model and bioprinted skin-like tissue: (i) Layer-by-layer skin model contained 10 layers of collagen, fibroblasts and keratinocytes, (ii) The immunofluorescent and bright field images of the skin-like tissue. Scale bars, 150 µm. Reproduced with permission [73]. Copyright 2009 Elsevier. **b** Schematic of 3D bioprinting and immunohistochemical staining of skin construct: (i) Schematic demonstration of the 3D bioprinting, consolidation and maturation steps using the developed bioink, (ii) Immunohistochemical staining of the bioprinted skin. Optical microscopy images of normal human skin and bioprinted skin after 26 days of culture. Reproduced with permission [76]. Copyright 2016 John Wiley and Sons

duction system is made of special cardiac fibers which can generate electrical impulse to trigger pulse of the cardiomyocytes [78].

Cardiovascular disease, cardiomyopathy and valvular disease are the major types of heart diseases [79]. Currently, the treatments of heart diseases strongly depend on cardiac stent, prosthetic heart valve and even heart transplantation. However, there are still plenty of shortcomings in clinical therapies [80]. The properties and structures of the constructed scaffold play vital roles in tissue engineering, since the scaffold should be identical to support the structure of heart tissue. Beyond that, choosing of cell types and vascularization of heart architectures are also big challenges. 3D bioprinting technology is a prospective solution to overcome the limitations of the current therapy, which can precisely assemble biomaterials with definite organization and spatial arrangements to mimic the native ECM environment of the cells [81]. The developments of 3D printed heart-like tissue are shown in Table 6.

Gaetani et al. created a porous scaffold by printing technique. In this system, human cardiac-derived cardiomyocytes progenitor cells (hCMPCs), the most promising cell source for heart regeneration, were homogeneously distributed in the fabricated scaffolds and retained a viability of 89% in 7 days [82]. It was indicated from the gene expression results of the early cardiac transcription factors that hCMPCs could retain their own characteristics in the resulting scaffold. Moreover, cell migration from alginate matrix to Matrigel

**Table 6** Bioinks for 3D bioprinted heart-like tissue

| Bioink materials | Cell sources | Printing types | Culture time | Outcomes |
|---|---|---|---|---|
| Alginate | hCMPCs | N/a | 7 days | Cells in the hydrogels retained high viability and commitment for cardiac lineage [82] |
| GelMA, alginate | HUVECs, cardiomyocytes | Laser-based | 14 days | Generating an endothelium myocardium for toxicity evaluation [83] |
| Alginate, gelatin | SMCs, VICs | Extrusion-based | 7 days | Fabricating aortic valve conduit with SMCs in the valve root and VIC in the leaflet [84] |
| PEUU | HUVECs, MSCs | Droplet-based | 8 days | The cardiac path in the rat led to increased vessel formation and improved function [85] |

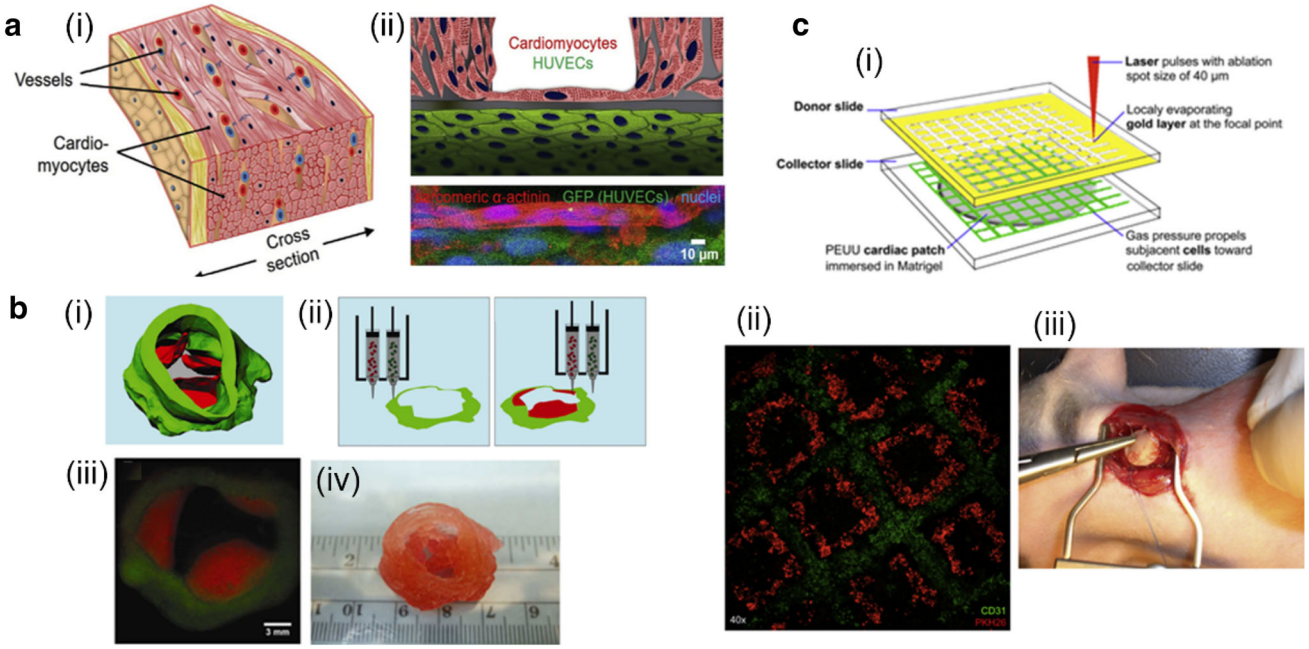


**Fig. 5** 3D bioprinting of heart-like tissue. **a** Schematic and confocal microscope images of the cardiomyocytes: (i) Structure of myocardial tissue with blood vessels implanted in the matrix, (ii) Schematic and immunofluorescence image of an endothelialized cardiomyocytes. Scale bar, 10 μm. Reproduced with permission [83]. Copyright 2016 Elsevier. **b** Structure of bioprinted aortic valve conduit: (i) Micro-CT image of aortic valve model, (ii) Operational demonstration of the bioprinting technique with dual channels which contained different cell types, (iii) The fluorescent image of the bioprinted aortic valve conduit with red-stained SMCs in the valve root and green-stained VICs in the valve leaflet. Scale bar, 3 mm, (iv) Printed aortic valve conduit. Reproduced with permission [84]. Copyright 2012 John Wiley and Sons. **c** LIFT based on PEUU patterns and cardiac patch in vitro and in vivo: (i) The diagram of cardiac patch's formation, (ii) Immunofluorescence image of cardiac patch, the MSCs and patches were separately stained by PKH26 and CD31 after 24 h of culture, (iii) Infracted heart region of rat with cardiac patch implantation. Reproduced with permission [85]. Copyright 2011 Elsevier

substrates resulted in the formation of tubular structures [82]. Zhang et al. utilized bioprinting method to fabricate an endothelium layer in which HUVECs and cardiomyocytes were embedded within GelMA and alginate hybrid hydrogel. It was found that the artificial myocardium structure was able to spontaneously and synchronously contract. Furthermore, the fabricated scaffold was placed into a microfluidic perfusion bioreactor for toxicity evaluation (Fig. 5a) [83].

Duan et al. successfully printed valve conduits composed of alginate-gelatin hybrid hydrogel (Fig. 5b). Aortic root sinus smooth muscle cells (SMCs) and aortic valve leaflet interstitial cells (VICs) were encapsulated in valve roots and leaflets of the printed valve conduits, respectively [84]. Gaebel et al. used Laser-Induced-Forward-Transfer (LIFT) cell printing technique to deposit MSCs and HUVECs on a polyester urethane urea (PEUU) cardiac patch (Fig. 5c) [85]. The majority of HUVECs were connected as the defined pattern after 8 days of in vitro culture. The results demonstrated that the cardiac patch transplanted into a rat could promote vascularization of the infarcted heart. This study provided both theoretical and practical foundation for the cardiac regeneration technology [85]. On the other hand, 3D

bioprinting tissue engineering can fabricate heart valve with high-resolution structure which has the ability to integrate with host tissues and grow within the body [86].

## Bioprinting of liver

The liver is a key organ in human body, which performs more than 500 functions in metabolic homeostasis including synthesis, secretion, storage, metabolism and detoxification [87]. Liver tissue has unique regenerative ability to recover its function and original volume even after 70% of partial hepatectomy [88]. On a microstructural level, the functional unit of liver is hepatic lobule, which carries on the crucial functions of secretion and detoxification [5]. At the cellular level, the main functional or parenchymal cells of the liver are hepatocytes accounting for approximately 80% of liver mass [89]. The nonparenchymal cells of the liver with structural and supportive functions are composed of portal fibroblasts, sinusoidal endothelial cells (SECs), biliary epithelial cells, hepatic stellate cells (HSCs), stromal cells and Kupffer cells (KCs).

Among numerous techniques to fabricate biomimetic liver tissues, 3D bioprinting provides the great potential with complex structures, high cell density and high cell–cell adhesion. To better mimic liver-specific ECM components, bioink applied for liver tissue fabrication should match the microenvironment of liver. The proportion of ECM materials in liver tissue is approximately 3% of the liver area, which is particularly lower than some other organs in human body [90]. In addition, the mechanical properties of ECM-mimicking biomaterials play a key role in modulating activation of HSCs [91]. As shown in Table 7, numerous studies on the 3D printed liver organoids or organs-on-a-chip were carried out around toxicology testing and drug metabolism, since liver was the important organ for detoxification.

Chang et al. [92] developed a liver micro-organ device for biomimetic drug metabolic studies, in which human hepatocellular carcinoma cells (HepG2) were encapsulated within alginate hydrogel. Bhise et al. [93] constructed a liver-on-a-chip platform of 3D printed hepatic spheroids for drug toxicity assessment, which could maintain its function after 30 days of culture. Matsusaki et al. [94] constructed hierarchical liver tissue micro-arrays using HepG2/HUVECs-laden fibronectin and gelatin. The fabricated 3D-human liver chips showed high cell activities and high cell–cell interactions, because the hierarchical sandwich structures were analogous to the native liver structure [94]. In the work by Ma et al. [95] it was found that the functions of liver tissue were closely related to the 3D assembly of hepatocytes with the supporting cell types. A triculture hepatic model, comprised of human induced pluripotent stem cells (hiPSCs) derived hepatic progenitor cells, HUVECs and adipose-derived stem cells, was developed in a microscale hexagonal architecture by rapid 3D bioprinting technology (Fig. 6a) [95]. After 20 days of culture, the constructed triculture model exhibited improved morphological organization, high liver-specific gene expression levels, increased secre-

**Table 7** Bioinks for 3D bioprinted liver tissue

| Bioink materials | Cell sources | Printing types | Culture time | Outcomes |
|---|---|---|---|---|
| Alginate | HepG2 | Extrusion-based | 1 week | Developing a liver micro-organ device as an in vitro drug metabolism model [92] |
| GelMA | HepG2/C3A cells | Droplet-based | 30 days | Developing a liver-on-a-chip platform of 3D printed hepatic spheroids for drug toxicity assessment [93] |
| Fibronectin, gelatin | HepG2, HUVEC | Droplet-based | 7 days | Constructing hierarchical HepG2 tissue micro-arrays [94] |
| GelMA | hiPSCs, HUVECs, adipose-derived stem cells | Digital light processing (DLP)-based | 20 days | The constructed triculture model exhibited improved morphological organization, high liver-specific gene expression levels, increased secretion of metabolic product, and enhanced cytochrome P450 induction [95] |
| NovoGel | Primary human hepatocytes, HSCs, HUVECs | Extrusion-based | 28 days | Establishing a novel bioprinted human mini liver tissue to test clinical drug-induced toxicity *in vitro* [96] |
| Matrigel | HepG2 | Extrusion-based | N/a | Combining 3D cell printing and microfluidic device [97] |
| Gelatin | Hepatocytes | Extrusion-based | 2 months | The laminated hepatocytes remained viable and performed biological functions for more than 2 months [98] |

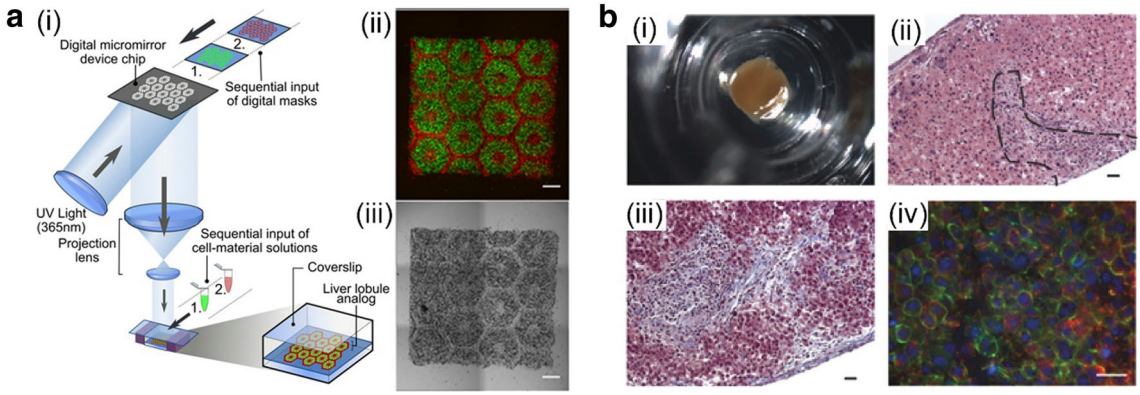


**Fig. 6** 3D bioprinting of liver constructs. **a** bioprinted hepatic construct: (i) Schematic diagram of a two-step 3D bioprinting approach, (ii–iii) Images (5×) taken under fluorescent and bright field channels showing patterns of fluorescently labeled hiPSC-HPCs (green) and supporting cells (red) on day 0. Scale bars, 500 μm. Reproduced with permission [95]. Copyright 2016 National Academy of Sciences. **b** Images of Organovo's mini liver tissue: (i) A macroscopic image of liver tissue housed in a 24 well transwell, (ii) H&E staining of a tissue cross-section, (iii) ECM deposition assessed by Masson's trichrome staining, (iv) IHC staining of the parenchymal compartment for E-cadherin (green) and Albumin (red). Reproduced with permission [96]. Open Access

tion of metabolic product and enhanced cytochrome P450 induction [95].

Notably, Nguyen et al. [96] established a novel bioprinted human mini liver tissue composed of primary human hepatocytes, HSC and HUVEC cells to test clinical drug-induced toxicity in vitro, which is the first report of mimicking human drug response at tissue level (Fig. 6b). It was demonstrated that the liver tissue retained ATP and Albumin levels as well as expression and drug-induced enzyme activity of Cytochrome P450s after 28 days post-fabrication [96]. Snyder et al. [97] utilized Matrigel for printing of a liver-like tissue in a microfluidic chip for radioprotection study. In the study by Wang et al. [98], it was found that the laminated hepatocytes remained viable and performed biological functions for more than 2 months.

## Bioprinting of neural tissues

The functional loss of central and peripheral nervous systems is usually caused by traumatic injuries and chronic degenerative diseases, which has severe impact on the life quality of patients (e.g., life-long disability and neuropathic pain) around the world [99,100]. In the case of nerve repair, the axons serving as nerve signal conducting fibers should be recovered or reconnected from the injury site. In fact, the chance for satisfactory recovery of motor function is only 40% in statistic [101], because of a nerve bundle containing thousands of axons. Moreover, therapeutics for bridging injured nerve gaps and recovering of neural function are still in very early stages. Fortunately, 3D bioprinting, using suitable bioinks and autogenous cells to from a mimetic tissue construct, provides a promising solution in neural tissue repair and regeneration. An ideal neural bioink should meet numerous requirements including biocompatibility, biodegradability, suitable mechanical properties, electrical conductivity for neural communication, as well as permeability for exchange of nutrients and waste [102,103]. Moreover, the features of minimizing cell settling and aggregation and sustained release of nerve growth factor are also key elements for bioprinting of neural constructs.

In the aspect of axons regeneration, Schwann cells (SCs) are the most common types of supporting cells. Because of the limited availability of SCs, there are also some alternative cell types, including BMSCs, hair follicle stem cells, olfactory ensheathing cells, adipose- and skin- derived stem cells [100]. In biofabrication of neural tissues, the optimal cell types involved are neural stem cells, mesenchymal stem cells (MSCs) and induced pluripotent stem cells [104], due to their capacity to differentiate into any neural cell type [105]. As demonstrated in Table 8, over the last years, several materials have been developed for bioprinting of neural constructs.

Lee et al. developed a neural tissue construct based on collagen and fibrin hydrogels laden with murine neural stem cells (C17.2) and VEGF. The results illustrated growth factor-induced cell migration and proliferation [106]. In the work by Ferris et al. shown in Fig. 7a, neural (PC-12) and skeletal muscle (C2C12) cells were encapsulated within the low-acyl gellan gum by a droplet-based bioprinting technique [107]. After 8 days of culture, the construct exhibited the extension of dense neural networks from PC12 cells into surrounding areas populated by skeletal muscle cells. Furthermore, Gu et al. [108] bioprinted neural mini-tissues for the first time. In this construct, human neural stem cells (hNSCs) were embedded in alginate, carboxymethyl-chitosan and agarose bioink by extrusion-based bioprinting. After approximately 10 days post-printing, hNSCs were differentiated to func-

**Table 8** Bioinks for 3D bioprinted neural tissue

| Bioink materials | Cell sources | Printing types | Culture time | Outcomes |
|---|---|---|---|---|
| Collagen, fibrin | Murine neural stem cells (C17.2) | Droplet-based | 3 days | Growth factor-induced cell migration and proliferation [106] |
| Gellan gum | Neural cells (PC-12), skeletal muscle cells (C2C12) | Droplet-based | 8 days | Extension of dense neural networks into surrounding areas populated by skeletal muscle cells [107] |
| Alginate, chitosan, agarose | hNSCs | Extrusion-based | 3 weeks | Functional neurons and supporting neuroglia spontaneously showed an increased calcium response to bicuculline [108] |
| Agarose | BMSCs, SCs | Extrusion-based | 7 days | Demonstrating the recovery of motor and sensor function in a rat using the constructed nerve graft [109] |
| Collagen | Rat embryonic neurons and astrocytes | Droplet-based | 15 days | Aggressive neural cell growth and viability shown in neural construct [110] |
| Collagen, fibrin | Primary embryonic hippocampal, cortical and NT2 neurons | Droplet-based | 15 days | Evaluating neuronal phenotypes and electrophysiology of the created 3D neural sheets [111] |
| Gelatin | SCs, astroglial cells, pig lens epithelial cells | Laser-based | 2 weeks | Cells were able to survive, proliferate and differentiate after laser pulsed transfer [112] |
| PU | NSCs | Extrusion-based | 7 days | The bioprinted grafts were used in recovering nerve function in Zebrafish neural injury models [113] |

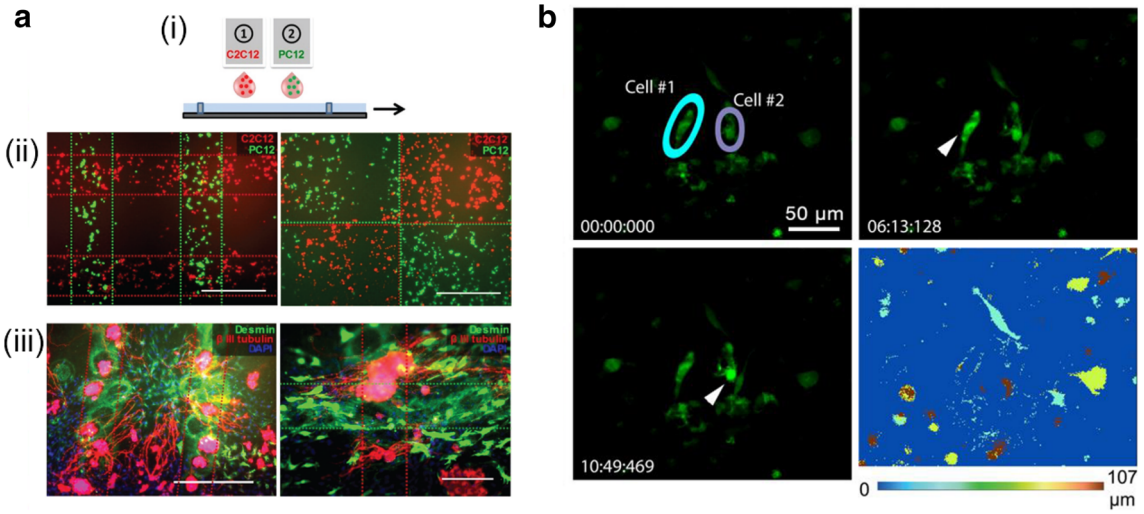


**Fig. 7** Fabrication of 3D neural tissue by bioprinting. **a** Patterning of two cell types printed simultaneously from two separate inkjet print heads onto collagen substrates: (i) Schematic representation of multiple head printing, (ii) C2C12 (red) and PC12 (green) cells pre-stained with CellTracker™ dyes and printed in various patterns. Images were taken 1 h after printing, following the addition of the culture medium, Scale bars, 500 μm, (iii) Printed patterns of C2C12 and PC12 cells after 8 days under differentiation conditions. Cells were immunostained for desmin (C2C12, green) and β-III tubulin (PC12, red). Reproduced with permission [107]. Copyright 2012 Royal Society of Chemistry. **b** Time course of live calcium imaging of neurons within a 3D construct, with the bottom right panel showing depth coding of cells along the *Z*-axis (0–107 μm). Arrowheads indicate active cells. Reproduced with permission [108]. Copyright 2016 John Wiley and Sons

tional neurons and supporting neuroglia. The differentiated neurons exhibited synaptic contacts and network formation and spontaneously showed an increased calcium response to bicuculline (Fig. 7b) [108]. On the other hand, the capacity of bioprinted nerve grafts has been investigated in recovering sensory and motor function. Owens *et al.* employed bioprinting to fabricate a nerve graft composed of BMSCs, SCs and agarose. The agarose rods were used as supporting materials and removed after 7 days. Importantly, both motor and sensory function in a rat sciatic nerve injury model were recovered after 40 weeks of implantation of the constructed neural grafts [109].

Lee et al. 3D bioprinted a neural tissue model in which rat embryonic neurons and astrocytes were embedded within collagen. After 15 days of culture, aggressive neural cell growth and viability were observed in the printed neural construct [110]. Xu et al. used collagen and fibrin laden with primary embryonic hippocampal, cortical and NT2 neurons to fabricate 3D neural sheets. The neuronal phenotypes and electrophysiology of the printed construct were evaluated [111]. In the study by Hopp et al. different cell types of SCs, astroglial cells and pig lens epithelial cells were deposited into gelatin. It was illustrated that the cells were able to survive, proliferate and differentiate after laser pulsed transfer [112]. Additionally, Hsieh and Hsu [113] developed a nerve graft made of NSCs-laden polyurethane (PU), which was successfully used in recovering nerve function in Zebrafish neural injury models.

## Future perspectives

### Novel bioink materials

Although the development of a wide range of printable materials has achieved a big advance, the majority of existing bioink materials are far from perfect to retain cell viability, spreading and proliferation during long-time culture, furthermore to establish cell–cell and cell–matrix interactions and eventually functionalize the printed tissue constructs. Naturally derived hydrogels usually have poor mechanical properties, therefore cannot build large architectures without additional support. While synthetic hydrogels generally have limited biological interactions, such as lack of motifs for cell adhesion or migration. At this point, supramolecular hydrogels formed through noncovalent interactions, including hydrogen bonding, π–π stacking, van der Waals, electrostatic and hydrophobic interactions [114], cause concerns of 3D bioprinting as an alternative new kind of bioink candidates [115]. In comparison with chemically cross-linked polymeric hydrogels, supramolecular hydrogels possess numerous merits, including biocompatibility, biodegradability, environmental stimuli responsibility, ordered and reversible structures, controllable self-assembly, easy modification and tunable bioactive behaviors [115,116]. In particular, peptide-based hydrogels have the most potential to become bioink candidates in tissue fabrication, because their structural and functional properties can be easily regulated by varying amino acid types, sequences and numbers [116].

### Cell type and density

In the future, the prospect of using patient autogenous cells to construct living and functional tissues will provide revolutionary changes in the fields of research and healthcare. However, in the aspect of placing and culturing cells in 3D space, there still exist numerous challenges, such as cell types and density, the spatial arrangement and local microenvironment [117]. From the perspective of tissue engineering, the threshold of cell density for solid organ replacement was at 1–10 billion of function cells [117]. The current status is far from the target. It has been observed many years ago that "…gels seeded with cells have been limited by the fact that the resultant cell densities per unit volume that can be achieved are much lower than those observed in vivo…" [118]. Until now however, maintaining and improving cell density in tissue construct is still an unsolved problem [119]. When planning for a tissue or organoid fabrication, we should figure out how to organize multiple cell types into spatial arrangement where their original function can be achieved in the post-printing tissue maturation period.

### Vascularization

In the field of tissue engineering, vascularization is widely regarded as one of the key preconditions to applications in vivo [29]. It has been found that the location of cells more than 200 μm away from the nearest capillaries will undergo hypoxia, apoptosis and death, due to the internal mass transfer limitations [120]. Therefore, within the 3D bioprinted tissues or organs, implement of vascularization is crucial for penetrations of oxygen and nutrients as well as long-term maintenance of tissue functions [121]. The vascularization will greatly contribute to the solution of maintaining high cell viability and functionality in 3D bioprinted complex and large-volume tissue constructs, but there's still a long way to go.

**Acknowledgements** The authors acknowledge financial support from the National Natural Science Foundation of China (Project No. 21703253, 21774132, 21644007) and the Talent Fund of the Recruitment Program of Global Youth Experts.

## References


1. Ozbolat IT, Yu Y (2013) Bioprinting toward organ fabrication: challenges and future trends. IEEE Trans Bio-Med Eng 60(3):691–699
2. Lee JM, Yeong WY (2016) Design and printing strategies in 3D bioprinting of cell-hydrogels: a review. Adv Healthc Mater 5(22):2856–2865
3. Mir TA, Nakamura M (2017) 3D-Bioprinting: towards the era of manufacturing human organs as spare parts for healthcare and medicine. Tissue Eng Part B Rev 23(3):245–256
4. Gauvin R, Chen YC, Jin WL, Soman P, Zorlutuna P, Nichol JW, Bae H, Chen S, Khademhosseini A (2012) Microfabrication of complex porous tissue engineering scaffolds using 3D projection stereolithography. Biomaterials 33(15):3824–3834
5. Zhang YS, Yue K, Aleman J, Mollazadehmoghaddam K, Bakht SM, Yang J, Jia W, Dell'Erba V, Assawes P, Shin SR (2017) 3D bioprinting for tissue and organ fabrication. Ann Biomed Eng 45(1):148–163
6. Kengla C, Atala A, Sang JL (2015) Chapter 15-bioprinting of organoids. In: Haley M (ed) Essentials of 3D biofabrication and translation. Elsevier Inc, USA
7. Chang R, Nam Y, Sun W (2008) Direct cell writing of 3D microorgan for in vitro pharmacokinetic model. Tissue Eng Part C-Methods 14(2):157–166
8. Dababneh AB, Ozbolat IT (2014) Bioprinting technology: a current state-of-the-art review. J Manuf Sci Eng 136(6):061016
9. Ozbolat IT, Hospodiuk M (2016) Current advances and future perspectives in extrusion-based bioprinting. Biomaterials 76(37):321–343
10. Gudapati H, Dey M, Ozbolat I (2016) A comprehensive review on droplet-based bioprinting: past, present and future. Biomaterials 102:20–42
11. Schiele NR, Corr DT, Huang Y, Raof NA, Xie Y, Chrisey DB (2010) Laser-based direct-write techniques for cell printing. Biofabrication 2(3):032001
12. Hospodiuk M, Dey M, Sosnoski D, Ozbolat IT (2017) The bioink: a comprehensive review on bioprintable materials. Biotechnol Adv 35(2):217–239
13. Yao X, Peng R, Ding JD (2013) Cell-material interactions revealed via material techniques of surface patterning. Adv Mater 25(37):5257–5286
14. Jungst T, Smolan W, Schacht K, Scheibel T, Groll J (2016) Strategies and molecular design criteria for 3D printable hydrogels. Chem Rev 116(3):1496–1539
15. Yu L, Ding JD (2008) Injectable hydrogels as unique biomedical materials. Chem Soc Rev 37(8):1473–1481
16. Ahmed EM (2015) Hydrogel: preparation, characterization, and applications: a review. J Adv Res 6(2):105–121
17. Marchant RE (2011) Design properties of hydrogel tissue-engineering scaffolds. Expert Rev Med Devices 8(5):607–626
18. Alakpa E, Jayawarna V, Lampel A, Burgess K, West C, Bakker SJ, Roy S, Javid N, Fleming S, Lamprou D (2016) Tunable supramolecular hydrogels for selection of lineage-guiding metabolites in stem cell cultures. Chem 1(2):298–319
19. Discher DE, Janmey P, Wang YL (2005) Tissue cells feel and respond to the stiffness of their substrate. Science 310(5751):1139–1143
20. Wells RG (2008) The role of matrix stiffness in regulating cell behavior. Hepatology 47(4):1394–1400
21. Lutolf MP, Weber FE, Schmoekel HG, Schense JC, Kohler T, Müller R, Hubbell JA (2003) Repair of bone defects using synthetic mimetics of collagenous extracellular matrices. Nat Biotechnol 21(5):513–518
22. Richardson TP, Peters MC, Ennett AB, Mooney DJ (2001) Polymeric system for dual growth factor delivery. Nat Biotechnol 19(11):1029–1034
23. Malda J, Visser J, Melchels FP, Jüngst T, Hennink WE, Dhert WJ, Groll J, Hutmacher DW (2013) 25th Anniversary article: engineering hydrogels for biofabrication. Adv Mater 25(36):5011–5028
24. Murphy SV, Aleksander S, Anthony A (2013) Evaluation of hydrogels for bio-printing applications. J Biomed Mater Res, Part A 101(1):272–284
25. Carrow JK, Kerativitayanan P, Jaiswal MK, Lokhande G, Gaharwar AK (2015) Chapter 13-polymers for bioprinting. In: Haley M (ed) Essentials of 3D biofabrication and translation. Elsevier Inc, USA
26. Burdick JA, Chung C, Jia X (2005) Controlled degradation and mechanical behavior of photopolymerized hyaluronic acid networks. Biomacromolecules 6(1):386–391
27. Wu LB, Ding JD (2004) In vitro degradation of three-dimensional porous poly(D, L-lactide-co-glycolide) scaffolds for tissue engineering. Biomaterials 25(27):5821–5830
28. Khalil S, Sun W (2009) Bioprinting endothelial cells with alginate for 3D tissue constructs. Trans ASME J Biomech Eng 131(11):111002
29. Malheiro A, Wieringa P, Mota C, Baker M, Moroni L (2016) Patterning vasculature: the role of biofabrication to achieve an integrated multicellular ecosystem. ACS Biomater Sci Eng 2(10):1694–1709
30. Melchiorri AJ, Fisher JP (2015) Chapter 20-bioprinting of blood vessels. In: Haley M (ed) Essentials of 3D biofabrication and translation. Elsevier Inc, USA
31. Murphy SV, Atala A (2014) 3D bioprinting of tissues and organs. Nat Biotechnol 32(8):773–785
32. Muschler GF, Nakamoto C, Griffith LG (2004) Engineering principles of clinical cell-based tissue engineering. J Bone Joint Surg 86–A:1541–1558
33. Norotte C, Marga FS, Niklason LE, Forgacs G (2009) Scaffold-free vascular tissue engineering using bioprinting. Biomaterials 30(30):5910
34. Lu HJ, Feng ZQ, Gu ZZ, Liu CJ (2009) Growth of outgrowth endothelial cells on aligned PLLA nanofibrous scaffolds. J Mater Sci-Mater Med 20(9):1937–1944
35. Xu C, Chai W, Huang Y, Markwald RR (2012) Scaffold-free inkjet printing of three-dimensional zigzag cellular tubes. Biotechnol Bioeng 109(12):3152–3160
36. Miller JS, Stevens KR, Yang MT, Baker BM, Nguyen DH, Cohen DM, Toro E, Chen AA, Galie PA, Yu X, Chaturvedi R, Bhatia SN, Chen CS (2012) Rapid casting of patterned vascular networks for perfusable engineered three-dimensional tissues. Nat Mater 11(9):768–774
37. Bertassoni LE, Cecconi M, Manoharan V, Nikkhah M, Hjortnaes J, Cristino AL, Barabaschi G, Demarchi D, Dokmeci MR, Yang Y, Khademhosseini A (2014) Hydrogel bioprinted microchannel networks for vascularization of tissue engineering constructs. Lab Chip 14(13):2202–2211
38. Fan R, Piou M, Darling E, Cormier D, Sun J, Wan J (2016) Bioprinting Cell-laden Matrigel-agarose Constructs. J Biomater Appl 31(5):684–692
39. Bertassoni LE, Cardoso JC, Manoharan V, Cristino AL, Bhise NS, Araujo WA, Zorlutuna P, Vrana NE, Ghaemmaghami AM, Dokmeci MR, Khademhosseini A (2014) Direct-write bioprinting of cell-laden methacrylated gelatin hydrogels. Biofabrication 6(2):024105
40. Skardal A, Zhang J, McCoard L, Xu X, Oottamasathien S, Prestwich GD (2010) Photocrosslinkable Hyaluronan-gelatin hydrogels for two-step bioprinting. Tissue Eng Part A 16(8):2675–2685

41. Salgado AJ, Coutinho OP, Reis RL (2004) Bone Tissue engineering: state of the art and future trends. Macromol Biosci 4(8):743–765
42. Knothe MLT (2003) Whither flows the fluid in bone? An osteocyte's perspective. J Biomech 36(10):1409–1424
43. Hing KA (1825) Bone repair in the twenty-first century: biology, chemistry or engineering? Philos Trans 2004(362):2821–2850
44. Larsen M, Mishra R, Miller M, Dean D (2015) Chapter 17-bioprinting of bone. In: Haley M (ed) Essentials of 3D biofabrication and translation. Elsevier Inc, USA
45. Sun W, Puzas JE, Sheu TJ, Liu X, Fauchet PM (2007) Nano- to microscale porous silicon as a cell interface for bone-tissue engineering. Adv Mater 19(7):921–924
46. Fedorovich NE, De Wijn JR, Verbout AJ, Alblas J, Dhert WJ (2008) Three-dimensional fiber deposition of cell-laden, viable, patterned constructs for bone tissue printing. Tissue Eng Part A 14(1):127–133
47. Gruene M, Deiwick A, Koch L, Schlie S, Unger C, Hofmann N, Bernemann I, Glasmacher B, Chichkov B (2011) Laser printing of stem cells for biofabrication of scaffold-free autologous grafts. Tissue Eng Part C Methods 17(1):79–87
48. Byambaa B, Annabi N, Yue K, Trujillo-de Santiago G, Alvarez MM, Jia W, Kazemzadeh-Narbat M, Shin SR, Tamayol A, Khademhosseini A (2017) Bioprinted osteogenic and vasculogenic patterns for engineering 3D bone tissue. Adv Healthc Mater 6(16):1700015
49. Keriquel V, Oliveira H, Remy M, Ziane S, Delmond S, Rousseau B, Rey S, Catros S, Amedee J, Guillemot F, Fricain JC (2017) In situ printing of mesenchymal stromal cells, by laser-assisted bioprinting, for in vivo bone regeneration applications. Sci Rep 7(1):1778
50. Fedorovich NE, Wijnberg HM, Dhert WJ, Alblas J (2011) Distinct tissue formation by heterogeneous printing of osteo- and endothelial progenitor cells. Tissue Eng Part A 17(15–16):2113–2121
51. Carlier A, Skvortsov GA, Hafezi F, Ferraris E, Patterson J, Koc B, Van Oosterwyck H (2016) Computational model-informed design and bioprinting of cell-patterned constructs for bone tissue engineering. Biofabrication 8(2):025009
52. Hung BP, Naved BA, Nyberg EL, Dias M, Holmes CA, Elisseeff JH, Dorafshar AH, Grayson WL (2016) Three-dimensional printing of bone extracellular matrix for craniofacial regeneration. ACS Biomater Sci Eng 2(10):1806–1816
53. Naumann A, Dennis JE, Awadallah A, Carrino DA, Mansour JM, Kastenbauer E, Caplan AI (2002) Immunochemical and mechanical characterization of cartilage subtypes in rabbit. J Histochem Cytochem Off Jo Histochem Soc 50(8):1049–1058
54. Umlauf D, Frank S, Pap T, Bertrand J (2010) Cartilage biology, pathology, and repair. Cell Mol Life Sci 67(24):4197–4211
55. Liu M, Zeng X, Ma C, Yi H, Ali Z, Mou X, Li S, Deng Y, He N (2017) Injectable hydrogels for cartilage and bone tissue engineering. Bone Res 5:17014
56. Cui X, Breitenkamp K, Finn MG, Lotz M, D'Lima DD (2012) Direct human cartilage repair using three-dimensional bioprinting technology. Tissue Eng Part A 18(11–12):1304–1312
57. Zhang YS, Yue K, Aleman J, Mollazadeh-Moghaddam K, Bakht SM, Yang J, Jia W, Dell'Erba V, Assawes P, Shin SR, Dokmeci MR, Oklu R, Khademhosseini A (2016) 3D bioprinting for tissue and organ fabrication. Ann Biomed Eng 45(1):148–163
58. Lai K, Xu T (2015) Chapter 18-bioprinting of cartilage: recent progress on bioprinting of cartilage. In: Haley M (ed) Essentials of 3D biofabrication and translation. Elsevier Inc, USA
59. Schuurman W, Levett PA, Pot MW, van Weeren PR, Dhert WJ, Hutmacher DW, Melchels FP, Klein TJ, Malda J (2013) Gelatin-methacrylamide hydrogels as potential biomaterials for fabrication of tissue-engineered cartilage constructs. Macromol Biosci 13(5):551–561
60. Park JY, Choi JC, Shim JH, Lee JS, Park H, Kim SW, Doh J, Cho DW (2014) A comparative study on collagen type I and hyaluronic acid dependent cell behavior for osteochondral tissue bioprinting. Biofabrication 6(3):035004
61. Daly AC, Critchley SE, Rencsok EM, Kelly DJ (2016) A comparison of different bioinks for 3D bioprinting of fibrocartilage and hyaline cartilage. Biofabrication 8(4):045002
62. Shi W, Sun M, Hu X, Ren B, Cheng J, Li C, Duan X, Fu X, Zhang J, Chen H, Ao Y (2017) Structurally and functionally optimized silk-fibroin-gelatin scaffold using 3D printing to repair cartilage injury in vitro and in vivo. Adv Mater 29(29):170189
63. Kundu J, Shim JH, Jang J, Kim SW, Cho DW (2015) An additive manufacturing-based PCL-alginate-chondrocyte bioprinted scaffold for cartilage tissue engineering. J Tissue Eng Regen Med 9(11):1286–1297
64. Pescosolido L, Schuurman W, Malda J, Matricardi P, Alhaique F, Coviello T, van Weeren PR, Dhert WJ, Hennink WE, Vermonden T (2011) Hyaluronic acid and dextran-based semi-IPN hydrogels as biomaterials for bioprinting. Biomacromolecules 12(5):1831–1838
65. Apelgren P, Amoroso M, Lindahl A, Brantsing C, Rotter N, Gatenholm P, Kolby L (2017) Chondrocytes and stem cells in 3D-bioprinted structures create human cartilage in vivo. PLoS ONE 12(12):e0189428
66. Stichler S, Bock T, Paxton N, Bertlein S, Levato R, Schill V, Smolan W, Malda J, Tessmar J, Blunk T, Groll J (2017) Double printing of hyaluronic acid/poly(glycidol) hybrid hydrogels with poly(epsilon-caprolactone) for MSC chondrogenesis. Biofabrication 9(4):044108
67. Rhee S, Puetzer JL, Mason BN, Reinhartking CA, Bonassar LJ (2016) 3D bioprinting of spatially heterogeneous collagen constructs for cartilage tissue engineering. ACS Biomater Sci Eng 2(10):1800–1805
68. Vijayavenkataraman S, Lu WF, Fuh JY (2016) 3D bioprinting of skin: a state-of-the-art review on modelling, materials, and processes. Biofabrication 8(3):032001
69. Bouwstra JA, Honeywell-Nguyen PL, Gooris GS, Ponec M (2003) Structure of the skin barrier and its modulation by vesicular formulations. Prog Lipid Res 42(1):1–36
70. Koch L, Michael S, Reimers K, Vogt PM, Chichkov B (2015) Chapter 13-bioprinting for skin. In: Geraghty F (ed) 3D bioprinting and nanotechnology in tissue engineering and regenerative medicine. Elsevier Inc, USA
71. Michael S, Sorg H, Peck CT, Koch L, Deiwick A, Chichkov B, Vogt PM, Reimers K (2013) Tissue engineered skin substitutes created by laser-assisted bioprinting form skin-like structures in the dorsal skin fold chamber in mice. PLoS ONE 8(3):e57741
72. Lineen E, Namias N (2008) Biologic dressing in burns. J Craniofac Surg 19(4):923–928
73. Lee W, Debasitis JC, Lee VK, Lee JH, Fischer K, Edminster K, Park JK, Yoo SS (2009) Multi-layered culture of human skin fibroblasts and keratinocytes through three-dimensional freeform fabrication. Biomaterials 30(8):1587–1595
74. Lee V, Singh G, Trasatti JP, Bjornsson C, Xu X, Tran TN, Yoo SS, Dai G, Karande P (2014) Design and fabrication of human skin by three-dimensional bioprinting. Tissue Eng Part C Methods 20(6):473–484
75. Cubo N, Garcia M, Del Canizo JF, Velasco D, Jorcano JL (2016) 3D bioprinting of functional human skin: production and in vivo analysis. Biofabrication 9(1):015006
76. Pourchet LJ, Thepot A, Albouy M, Courtial EJ, Boher A, Blum LJ, Marquette CA (2017) Human skin 3D bioprinting using scaffold-free approach. Adv Healthc Mater 6(4):1601101
77. Farrell MJ, Kirby ML (2001) Cell biology of cardiac development. Int Rev Cytol 202(202):99–158

78. Severs NJ (2000) The cardiac muscle cell. BioEssays 22(2):188–199
79. Gelb BD (2013) Recent advances in understanding the genetics of congenital heart defects. Curr Opin Pediatr 25(5):561–566
80. Silvestri A, Boffito M, Sartori S, Ciardelli G (2013) Biomimetic materials and scaffolds for myocardial tissue regeneration. Macromol Biosci 13(8):984–1019
81. Mironov V, Reis N, Derby B (2006) Review: bioprinting: a beginning. Tissue Eng 12(4):631–634
82. Gaetani R, Doevendans PA, Metz CH, Alblas J, Messina E, Giacomello A, Sluijter JP (2012) Cardiac tissue engineering using tissue printing technology and human cardiac progenitor cells. Biomaterials 33(6):1782–1790
83. Zhang YS, Arneri A, Bersini S, Shin SR, Zhu K, Goli-Malekabadi Z, Aleman J, Colosi C, Busignani F, Dell'Erba V, Bishop C, Shupe T, Demarchi D, Moretti M, Rasponi M, Dokmeci MR, Atala A, Khademhosseini A (2016) Bioprinting 3D microfibrous scaffolds for engineering endothelialized myocardium and heart-on-a-chip. Biomaterials 110:45–59
84. Duan B, Hockaday LA, Kang KH, Butcher JT (2013) 3D bioprinting of heterogeneous aortic valve conduits with alginate/gelatin hydrogels. J Biomed Mater Res A 101(5):1255–1264
85. Gaebel R, Ma N, Liu J, Guan J, Koch L, Klopsch C, Gruene M, Toelk A, Wang W, Mark P, Wang F, Chichkov B, Li W, Steinhoff G (2011) Patterning human stem cells and endothelial cells with laser printing for cardiac regeneration. Biomaterials 32(35):9218–9230
86. Filová E, Straka F, Mirejovský T, Masín J, Bacáková L (2009) Tissue-engineered heart valves. Physiol Res 58 Suppl 2(6):S141–158
87. Ji B, Fisher J, Nyberg SL (2011) Liver regeneration and tissue engineering. In: Bernstein HS (ed) Tissue engineering in regenerative medicine. Humana Press, USA
88. Song ZW, Gupta K, Ng IC, Xing JW, Yang YA, Yu H (2018) Mechanosensing in liver regeneration. Semin Cell Dev Biol 71:153–167
89. Michalopoulos GK, DeFrances MC (1997) Liver regeneration. Science 276(5309):60–66
90. Bedossa P, Paradis V (2003) Liver extracellular matrix in health and disease. J Pathol 200(4):504–515
91. Natarajan V, Harris EN (2017) Kidambi S (2017) SECs (sinusoidal endothelial cells), liver microenvironment, and fibrosis. Biomed Res Int 1:4097205
92. Chang R, Emami K, Wu HL, Sun W (2010) Biofabrication of a three-dimensional liver micro-organ as an in vitro drug metabolism model. Biofabrication 2(4):045004
93. Bhise NS, Manoharan V, Massa S, Tamayol A, Ghaderi M, Miscuglio M, Lang Q, Zhang YS, Shin SR, Calzone G, Annabi N, Shupe TD, Bishop CE, Atala A, Dokmeci MR, Khademhosseini A (2016) A liver-on-a-chip platform with bioprinted hepatic spheroids. Biofabrication 8(1):014101
94. Matsusaki M, Sakaue K, Kadowaki K, Akashi M (2013) Three-dimensional human tissue chips fabricated by rapid and automatic inkjet cell printing. Adv Healthc Mater 2(4):534–539
95. Ma XY, Qu X, Zhu W, Li YS, Yuan SL, Zhang H, Liu J, Wang PR, Lai CSE, Zanella F, Feng GS, Sheikh F, Chien S, Chen SC (2016) Deterministically patterned biomimetic human ipsc-derived hepatic model via rapid 3D bioprinting. Proc Nat Acad Sci USA 113(8):2206–2211
96. Nguyen DG, Funk J, Robbins JB, Crogan-Grundy C, Presnell SC, Singer T, Roth AB (2016) Bioprinted 3D primary liver tissues allow assessment of organ-level response to clinical drug induced toxicity in vitro. PLoS ONE 11(7):e0158674
97. Snyder JE, Hamid Q, Wang C, Chang R, Emami K, Wu H, Sun W (2011) Bioprinting cell-laden matrigel for radioprotection study of liver by pro-drug conversion in a dual-tissue microfluidic chip. Biofabrication 3(3):034112
98. Wang XH, Yan YN, Pan YQ, Xiong Z, Liu HX, Cheng B, Liu F, Lin F, Wu RD, Zhang RJ, Lu QP (2006) Generation of three-dimensional hepatocyte/gelatin structures with rapid prototyping system. Tissue Eng 12(1):83–90
99. Zhu W, Castro NJ, Zhang LG (2015) Chapter 14-nanotechnology and 3D bioprinting for neural tissue regeneration. In: Geraghty F (ed) 3D bioprinting and nanotechnology in tissue engineering and regenerative medicine. Elsevier Inc, USA
100. Owens C, Marga F, Forgacs G (2015) Chapter 23-bioprinting of nerve. In: Haley M (ed) Essentials of 3D biofabrication and translation. Elsevier Inc, USA
101. Moneim M, Omer G (1998) Clinical Outcome Following Acute Nerve Repair. Management of Peripheral Nerve Problems. 1998:414–419
102. Cunha C, Panseri S, Antonini S (2011) Emerging nanotechnology approaches in tissue engineering for peripheral nerve regeneration. Nanomed Nanotechnol Biol Med 7(1):50–59
103. Subramanian A, Krishnan UM, Sethuraman S (2009) Development of biomaterial scaffold for nerve tissue engineering: biomaterial mediated neural regeneration. J Biomed Sci 16(1):108
104. Chen JL, Yin Z, Shen WLA, Chen XA, Heng BC, Zou XAH, Ouyang HW (2010) Efficacy of hESC-MSCs in knitted silk-collagen scaffold for tendon tissue engineering and their roles. Biomaterials 31(36):9438–9451
105. Ladak A, Olson J, Tredget EE, Gordon T (2011) Differentiation of mesenchymal stem cells to support peripheral nerve regeneration in a rat model. Exp Neurol 228(2):242–252
106. Lee Y-B, Polio S, Lee W, Dai G, Menon L, Carroll RS, Yoo S-S (2010) Bio-printing of collagen and VEGF-releasing fibrin gel scaffolds for neural stem cell culture. Exp Neurol 223(2):645–652
107. Ferris CJ, Gilmore KJ, Beirne S, McCallum D, Wallace GG, Panhuis MIH (2013) Bio-ink for on-demand printing of living cells. Biomater Sci 1(2):224–230
108. Gu Q, Tomaskoviccrook E, Lozano R, Chen Y, Kapsa RM, Zhou Q, Wallace GG, Crook JM (2016) Functional 3D neural mini-tissues from printed gel-based bioink and human neural stem cells. Adv Healthc Mater 5(12):1429–1438
109. Owens CM, Marga F, Forgacs G, Heesch CM (2013) Biofabrication and testing of a fully cellular nerve graft. Biofabrication 5(4):045007
110. Lee W, Pinckney J, Lee V, Lee JH, Fischer K, Polio S, Park JK, Yoo SS (2009) Three-dimensional bioprinting of rat embryonic neural cells. NeuroReport 20(8):798–803
111. Xu T, Gregory CA, Molnar P, Cui X, Jalota S, Bhaduri SB, Boland T (2006) Viability and electrophysiology of neural cell structures generated by the inkjet printing method. Biomaterials 27(19):3580–3588
112. Hopp B, Smausz T, Kresz N, Barna N, Bor Z, Kolozsvari L, Chrisey DB, Szabo A, Nogradi A (2005) Survival and proliferative ability of various living cell types after laser-induced forward transfer. Tissue Eng 11(11–12):1817–1823
113. Hsieh FY, Hsu SH (2015) 3D bioprinting: a new insight into the therapeutic strategy of neural tissue regeneration. Organogenesis 11(4):153–158
114. Du X, Zhou J, Shi J, Xu B (2015) Supramolecular hydrogelators and hydrogels: from soft matter to molecular biomaterials. Chem Rev 115(24):13165
115. Dou XQ, Feng CL (2017) Amino acids and peptide-based supramolecular hydrogels for three-dimensional cell culture. Adv Mater 29(16):1604062
116. Fleming S, Ulijn RV (2014) Design of nanostructures based on aromatic peptide amphiphiles. Chem Soc Rev 43(23):8150
117. Miller JS (2014) The billion cell construct: will three-dimensional printing get us there? PLoS Biol 12(6):e1001882

118. Niklason LE, Langer RS (1997) Advances in tissue engineering of blood vessels and other tissues. Transpl Immunol 5(4):303–306
119. Miller JS, Stevens KR, Yang MT, Baker BM, Nguyen DH, Cohen DM, Toro E, Chen AA, Galie PA, Yu X (2012) Rapid casting of patterned vascular networks for perfusable engineered three-dimensional tissues. Nat Mater 11(9):768–774
120. Novosel EC, Kleinhans C, Kluger PJ (2011) Vascularization is the key challenge in tissue engineering. Adv Drug Deliv Rev 63(4–5):300–311
121. Jeyaraj R, Natasha G, Kirby G, Rajadas J, Mosahebi A, Seifalian AM, Tan A (2015) Vascularisation in regenerative therapeutics and surgery. Mater Sci Eng C Mater Biol Appl 54:225–238